

Modern experiments – ATLAS

P. Eerola^a

^aLund University, Experimental High Energy Physics,
P.O. Box 118, SE-22100 Lund, Sweden

March 20th, 2008.

1. Introduction – why new experiments?

The Standard Model of particle physics is a well tested theory. It has been thoroughly tested in particular with the four LEP experiments ALEPH, DELPHI, L3 and OPAL, which collected data at the LEP electron-positron collider from 1989 to 2000. The current high-energy frontier lies at Fermilab, where the Tevatron proton-antiproton collider provides the CDF and D0 experiments collisions at 2 TeV centre-of-mass energy. All the results from these two experiments are also in concordance with the Standard Model.

Why should we then look for something else? For the first, the mass generation mechanism of the Standard Model, the Higgs mechanism, has not been experimentally verified since the Higgs boson, which emerges from the Higgs mechanism, has not been found yet. Secondly, the Higgs sector becomes problematic when the theory is extrapolated to high energies. The Higgs mass acquires radiative corrections through virtual particle loops, and the higher the energy, the larger these corrections become, approaching finally the Planck scale, 10^{19} GeV. In order to cancel these radiative corrections, one would have to fine-tune the coefficients in front of these corrections with a very high precision in order to cancel mass terms from radiative corrections in such a way that only the bare mass, $\mathcal{O}(100)$ GeV remains. This is called the naturalness problem. Third, there is no natural explanation why the electroweak mass scale (the energy scale for the unification of the electromagnetic and weak forces, $\mathcal{O} = 100$ GeV), and the Planck scale (the scale in which gravitation becomes as strong as the other forces,

$\mathcal{O} = 10^{19}$ GeV), are so vastly different. This is called the hierarchy problem.

A possible solution, introduced originally to solve the naturalness problem, is to introduce supersymmetry, which is a symmetry between bosons and fermions. Supersymmetry predicts superpartners to all existing particles, boson partners to fermions and vice versa. The superpartners would automatically cancel the large radiative corrections to Higgs mass. Furthermore, the lightest supersymmetric particle, called the LSP, is stable in most of the supersymmetry models, and the LSP is actually the best candidate for the Dark Matter of the Universe, making 23% of the matter-energy density of the Universe. The known matter makes only 4% of the matter-energy density.

Our Universe was created in the Big Bang according to the standard cosmology. It is natural to assume that the same quantity of particles and antiparticles were existing in the primordial soup. Our present Universe seems to consist of only matter, so where did all the antiparticles disappear? A. Sakharov defined three conditions in 1967 which are required for the disappearance of the antiparticles in the early Universe: C and CP violation, baryon number violation, and interactions out of thermal equilibrium. LHC may shed light on the primordial CP violation, both by providing data for studying the Standard Model CP violation, and by providing access to possible CP-violating effects beyond the Standard Model. The best place to look for CP violation at LHC are the B -hadrons, but CP-violating effects could even be studied with other processes.

For an overview of the current experimental status in particle physics, and reviews over experimental methods, see Ref. [1].

2. The next generation of experiments: ATLAS at the Large Hadron Collider

2.1. The Large Hadron Collider, LHC

The Large Hadron Collider, LHC, is a proton-proton collider, designed to operate at a centre-of-mass energy of $\sqrt{s} = 14$ TeV, and at a design luminosity of $L = 1 \times 10^{34} \text{ cm}^{-2}\text{s}^{-1}$. The accelerator is located in the Large Electron Positron (LEP) Collider tunnel across the Swiss-French border, 100 m underground. The length of the tunnel is 27 km.

The proton beams are first accelerated step by step in smaller accelerators at CERN: Linear Accelerator LINAC2, Proton Synchrotron PS, and Super Proton Synchrotron SPS. The CERN accelerator complex is shown in Fig. 1. At the last stage before the LHC, at SPS, the beams are accelerated to 450 GeV before injection to LHC. Each of the two beams at LHC contain 2808 proton bunches, with a minimum distance of approximately 7 m in between. Each bunch contains about 1.15×10^{11} protons and has a length of a few centimeters. The proton beams collide with a rate of 40 MHz (every 25 ns). At the design luminosity, the average number of proton-proton collisions per bunch-bunch crossing is about 23. Most of the extra events, called "pile-up" events, are so-called minimum bias events, producing only low- p_T hadrons (below 0.5 GeV).

The proton beams are bent along the LHC ring by 1232 superconducting dipole magnets. At 7 TeV beam energy, these magnets have to produce a field of around 8.4 Tesla at a current of around 11,700 A. The magnets have two apertures, one for each of the counter-rotating beams. The magnetic field is arranged in such a way that the bending direction is opposite for the two beams. The construction of the dipole magnets is shown in Fig. 2. Each dipole magnet is 14.3 metres long. The magnets are kept superconducting by using superfluid helium at a temperature of 1.9 K.

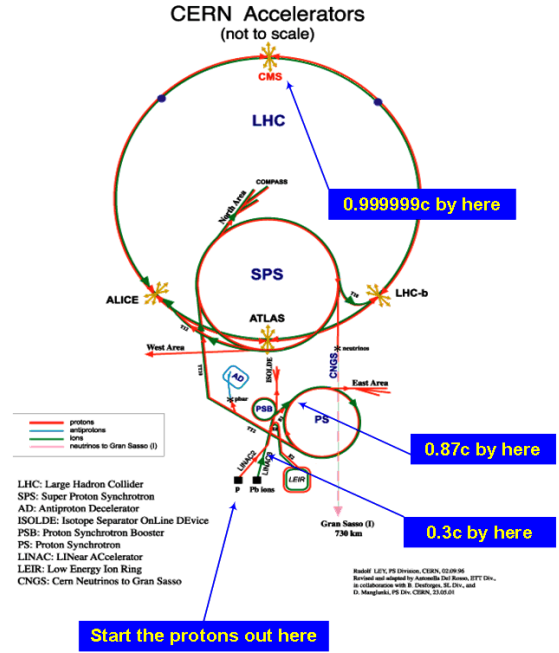


Figure 1. The CERN Accelerator Complex.

2.2. The ATLAS Experiment

ATLAS [2] is a general-purpose experiment at the Large Hadron Collider (LHC), with an emphasis on high- p_T physics beyond the Standard Model (SM). ATLAS has also capabilities for a rich B -physics programme, thanks to precise vertexing, tracking, high-resolution calorimetry, good muon identification, and a dedicated and flexible trigger scheme. Furthermore, ATLAS has a well-defined B -physics programme for all stages of the LHC-operation, from the commissioning run all the way up to the highest luminosity running at the LHC.

The ATLAS coordinate system is a right-handed system with the x -axis pointing to the centre of the LHC ring, the z -axis following the beam direction and the y -axis going upwards. The azimuthal angle $\phi = 0$ corresponds to the positive x -axis and ϕ increases clock-wise looking into the positive z direction. The polar angle θ is

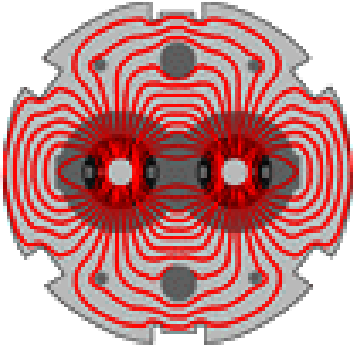


Figure 2. The LHC Dipole Magnet layout. The red lines show the magnetic field lines within the magnet and across the two beam pipes.

measured from the positive z -axis.

Transverse momentum p_T is defined as the momentum perpendicular to the LHC beam axis:

$$\vec{p}_T = \vec{p} \cos \theta \quad (1)$$

where \vec{p} is the three-momentum of the particle, and θ is the polar angle with respect to the beam-line.

Pseudorapidity is defined as

$$\eta = -\ln(\tan(\theta/2)) \quad (2)$$

The ATLAS detector is formed of three parts: The Inner Tracking Detector, which is located closest to the collision point, with a pseudorapidity coverage of $|\eta| < 2.5$; the calorimeter, composed of electromagnetic, hadronic, and forward sections and covering $|\eta| < 5$, and the magnetic muon spectrometer with $|\eta| < 2.7$. The ATLAS detector layout is shown in Fig. 3.

The Inner Detector comprises three subdetectors: Pixel, Semiconductor Tracker (SCT) and Transition Radiation Tracker (TRT). Each one is split into a barrel and two end-caps. The innermost part is the Pixel subdetector, consisting of 80 million rectangular silicon pixels of size $50 \mu\text{m} \times 400 \mu\text{m}$, leading to a resolution of $14 \mu\text{m}$ in $r\phi$ and $115 \mu\text{m}$ in the z -direction. They are organized in three barrel layers at radii of 5.0, 8.9,

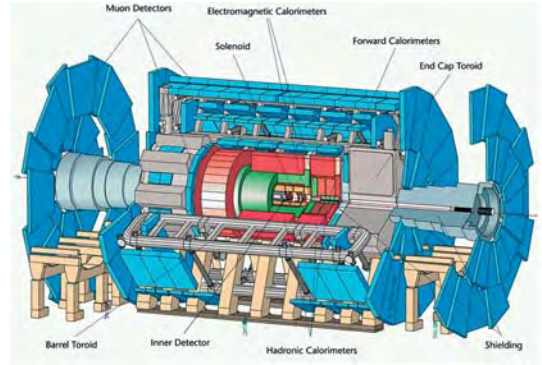


Figure 3. The ATLAS detector layout.

and 12.3 cm, respectively, and in three disks on either side. The Pixel sections are shown in Fig. 4.



Figure 4. The Pixel Barrel layers 1 and 2.

The Semiconductor Tracker (SCT) comprises four barrel layers of 153 cm length which are located between a radius of 30 cm and 51 cm. The detector elements are 6 cm long silicon strips with $80 \mu\text{m}$ pitch. The end-caps consist of nine disks of radius 56 cm, positioned up to $z = 2.8$ m.

The Transition Radiation Tracker (TRT) is the outermost element of the Inner Detector. A total

of 36 layers of straw tubes (4 mm in diameter and 150 cm in length) together with layers of radiator form the barrel. An individual straw tube has a resolution of $170\ \mu\text{m}$ and it is equipped with electronics with two thresholds in order to distinguish tracking hits from radiation hits for electron-pion separation.

A superconducting solenoid coil provides an axial magnetic field of 2 T along the beamline for the whole Inner Detector volume.

Figure 5 shows the insertion of the SCT and the TRT Barrel into the Barrel Calorimeter.



Figure 5. The insertion of the SCT and the TRT Barrel in the Barrel Calorimeter.

The Liquid Argon calorimeter is housed in a barrel and in two end-cap cryostats. The barrel contains the electromagnetic section, which is composed of 2 mm thick, accordion-shaped lead absorbers and electrodes with highly segmented read-out. In the end-cap region the same concept is used for the electromagnetic calorimeter, followed by a hadronic section with copper electrodes. The third element of the end-cap is the Forward Detector (outer radius of 45 cm), which consists of a section with copper absorber and two sections with tungsten as absorber.

The hadronic calorimeter is organized as a 564 cm long central barrel and two 290 cm long extended barrels. It uses iron plates as absorbers

and scintillators as active material. The read-out via fibres is segmented in elements in $\eta - \phi$ of 0.1×0.1 rad and in three compartments in depth.

The muon system consists of trigger chambers, precision chambers for measuring the tracks and the Toroid magnet system, again organized in a barrel part and two end-caps. The mechanical structure of the barrel is formed by the eight superconducting coils (25 m long, 5 m deep), interconnected by ribs as shown in Figure 6. One “wheel” of trigger chambers is shown in Fig. 7.

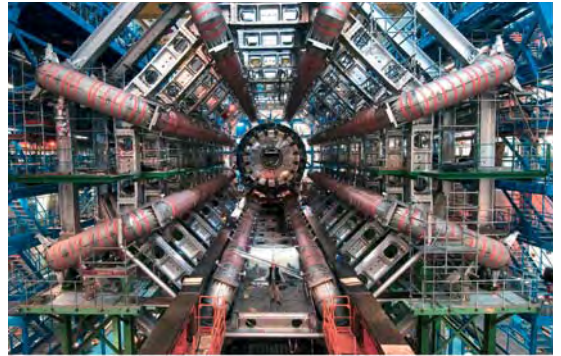


Figure 6. The coils of the Barrel Toroid Magnet with the Barrel Calorimeter.

3. Physics basics - luminosity, cross-sections, trigger

The event rate in particle collisions is given by

$$N = \sigma \times L \quad (3)$$

where σ is the cross-section of a physics process, and L is the instantaneous luminosity. The LHC design instantaneous luminosity is $L = 1 \times 10^{34}\ \text{cm}^{-2}\text{s}^{-1}$.

The integrated luminosity is given by

$$\mathcal{L} = \int L dt \quad (4)$$

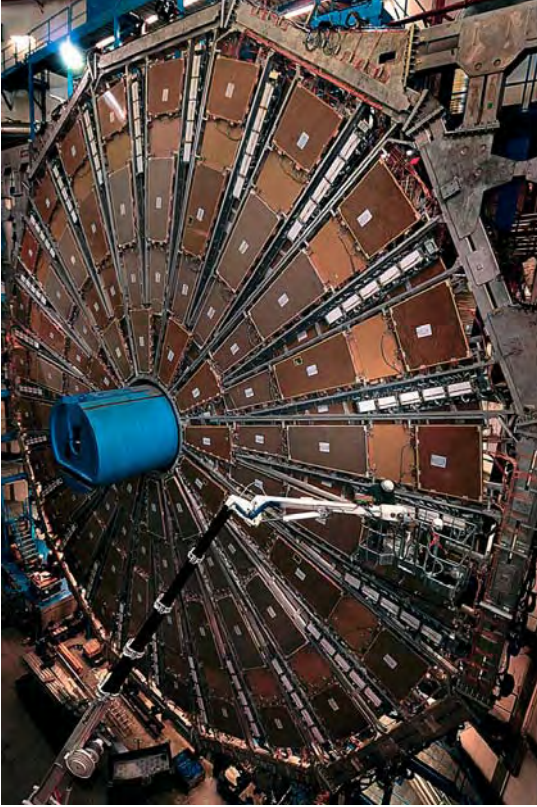


Figure 7. The End-Cap Muon Trigger chambers.

where L is the instantaneous luminosity and dt is the time. For example, an effective year is typically taken as 10^7 s (about 1/3 of a full year), since the accelerator cannot be operated continuously, but there are breaks and shut-downs for beam injection and for machine development. The integrated luminosity corresponding to running the accelerator at the design luminosity for an effective year is then:

$$\mathcal{L} = \int L dt = 10^{34} \text{ cm}^{-2}\text{s}^{-1} \times 10^7 \text{ s} = 100 \text{ fb}^{-1}$$

where

$$1 \text{ barn} = 1 \text{ b} = 10^{-24} \text{ cm}^2 \quad (5)$$

The number of events for an effective year is

then

$$N = \sigma \times \mathcal{L} \quad (6)$$

Figure 8 shows the cross-section, event rate, and number of events per year as a function of the particle mass at the LHC design centre-of-mass energy and design luminosity.

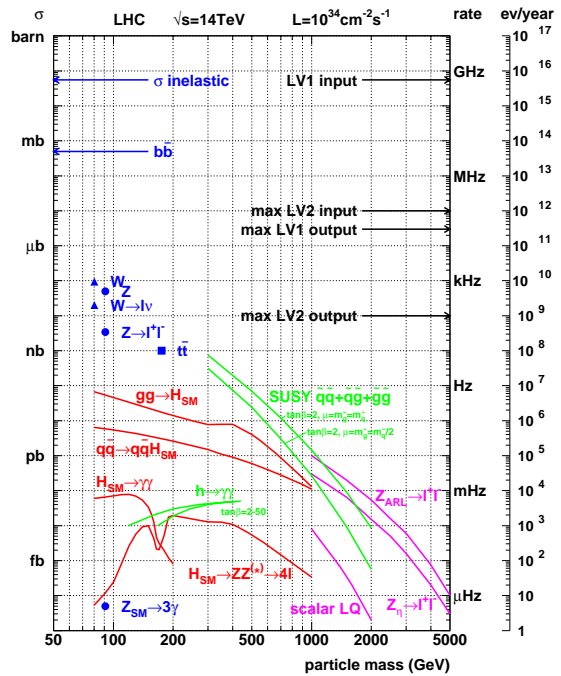


Figure 8. The cross-section, event rate, and number of events per year as a function of the particle mass at the LHC design centre-of-mass energy of $\sqrt{s} = 14$ TeV and design luminosity of $L = 1 \times 10^{34} \text{ cm}^{-2}\text{s}^{-1}$.

Using Equation 6, the number of $b\bar{b}$ events per year is thus:

$$N(b\bar{b}) = \sigma \times \mathcal{L} = 500 \mu\text{b} \times 100 \text{ fb}^{-1} = 10^{13} \text{ events}$$

We can also estimate the expected numbers of hypothetical new particles from the Fig.8, since one can predict the cross-sections of these new

particles as a function of the particle mass, and possibly fixing some free parameters. The number of Higgs events per year, assuming the Higgs mass being 200 GeV, and taking the four lepton decay mode, is:

$$\begin{aligned} N(H \rightarrow 4\ell) &= \sigma \times \mathcal{L} = 20 \text{ fb} \times 100 \text{ fb}^{-1} \\ &= 2000 \text{ events} \end{aligned}$$

The number of SUSY events per year, assuming $m(\text{squark}) = 300 \text{ GeV}$ and fixing some model parameters, is

$$\begin{aligned} N(\tilde{q}\tilde{q} + \tilde{q}\tilde{g} + \tilde{g}\tilde{g}) &= \sigma \times \mathcal{L} = 500 \text{ pb} \times 100 \text{ fb}^{-1} \\ &= 5 \times 10^7 \text{ events} \end{aligned}$$

There is, however, an evident problem here: we cannot collect all the data produced at LHC. The data can be written on disk with a typical maximum rate of 100-200 Hz, which means that at most $10^8 - 10^9$ events per year can be stored. Therefore a trigger system is needed. Triggering means selecting online those events which are interesting, and throwing away the uninteresting ones. The challenge is to design the trigger system in such a way that the system has as high efficiency as possible to the wanted signal events and as low efficiency as possible to the background events.

The ATLAS trigger system contains three levels which successively reduce the event rate from 40 MHz to 100-200 Hz. The level-1 is a hardware trigger based on high- p_T muon signals from the muon trigger chambers, high- E_T electron and photon signals from the electromagnetic calorimeters, high- E_T jet signals from the hadron calorimeters, and missing transverse energy signal obtained by summing up all the visible E_T seen in the calorimeters. The level-2 trigger is run on online processors, and is able to combine trigger signatures from different subdetectors. The highest trigger level, the event filter, reconstructs the whole event by combining data from all the subdetectors. The event filter runs on a computer farm.

High energy physics off-line data analysis starts from the raw data stored on a disk. The raw data, which is digital data from detector elements in local coordinates (*e.g.* 5 counts from wire number

25) is first converted to detector signals in a global geometry (*e.g.* a signal of 5 pC from a wire with a position $x=100 \text{ cm}$, $y=70 \text{ cm}$, $z=55 \text{ cm}$). For the conversion, calibration and geometry databases are needed. Then, a pattern recognition program tries to combine hits to particle trajectories in the tracking detectors or muon chambers, or to combine energy clusters to jet or electron/photon clusters in the calorimeters. Finally, an event reconstruction combines the particle trajectories and energy clusters into a complete event, from which one can try to figure out the original physical process.

One also needs simulated events in order to understand how the original signals look like in detectors with a certain resolution. In the Monte Carlo simulation process one goes the other way around: one starts with the physics process, follows the particle trajectories through the detector, simulates the physical processes occurring in the detectors (*e.g.* ionisation in the tracking detectors, shower formation in the calorimeters), and finally produces the simulated raw data.

4. Physics examples: Higgs, B -physics, black holes

4.1. Search for the Higgs boson

The Higgs mechanism, or something similar, is required to generate particle masses according to the Standard Model. The problem is that the Higgs particle itself has not yet been found, and the Standard Model as such does not predict the Higgs mass. The Higgs searches at LEP have put a lower limit for the Higgs mass at 115 GeV since the Higgs was not found at LEP. Furthermore, one can combine all the Standard Model precision measurements from LEP and Tevatron in order to estimate the most probable Higgs mass. This is possible, since the Higgs mass indirectly affects the measurable particle masses through virtual loops. These virtual loop corrections are most significant for the heaviest particles, the top-quark and the W - and Z -bosons. Figure 9 shows the probability as a function of the Higgs mass as derived from the combined Standard Model precision measurements. Figure 10 shows the mass of the W boson versus the mass of the top quark,

overlaid with the allowed Higgs mass bands. It is interesting to note that the current measurements of W boson and top quark masses favour a Minimal Supersymmetric Standard Model (MSSM) Higgs.

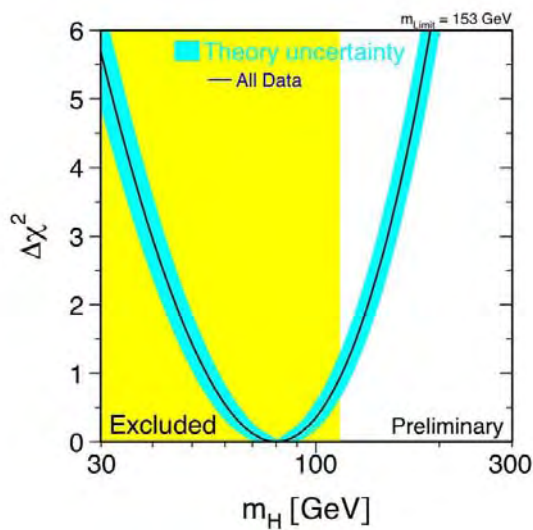


Figure 9. The χ^2 probability for the Higgs mass derived from Standard Model precision measurements. The lower the χ^2 , the larger the probability. The yellow region is the mass region excluded by LEP.

At LHC, the dominant process for producing a Higgs is gluon-gluon interaction which produces a Higgs via intermediate virtual top quarks, see Fig. 11. The Higgs coupling to bosons and fermions is related to their mass, so the Higgs is both produced by, and decays to preferably to heaviest possible particles.

Below Higgs mass of 130 GeV, the dominant Higgs decay is the decay to a b -quark pair. This decay mode is, however, very difficult to trigger on. Therefore one will instead be looking for the Higgs in alternative decay modes: $H \rightarrow \gamma\gamma$, $qqH \rightarrow qq\tau\tau$, $qqH \rightarrow qqWW$, $t\bar{t}H \rightarrow t\bar{t}b\bar{b}$. These

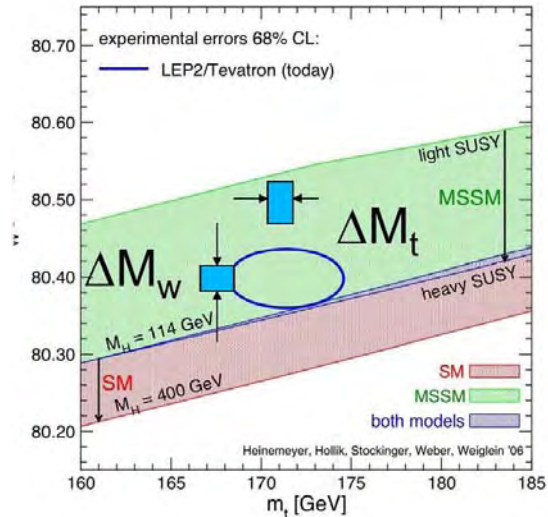


Figure 10. The measured W -mass (y -axis) versus the measured top mass (x -axis), and the Higgs mass bands. The red band shows the W -mass versus the top-mass band for a Standard Model Higgs; the upper edge of the band corresponds to a Higgs mass of 114 GeV, and the lower edge corresponds to a Higgs mass of 400 GeV. The green band shows the W -mass versus the top mass in the Minimum Supersymmetric Standard Model with five Higgs particles. In this case, the lightest of these five Higgs particles would play the same role as the Standard Model Higgs.

decay modes are possible to trigger on thanks to isolated photons (first decay mode), isolated taus (second decay), and high- p_T leptons (leptonic decays of W 's in the third case, and semileptonic decays of the top-quarks in the fourth case). Beyond Higgs mass of 130 GeV, dominant decay modes are $H \rightarrow ZZ^{(*)}$ (Z^* stands for an off-shell Z boson, *i.e.* a virtual Z boson with a mass below the nominal Z -boson mass of 91.2 GeV), $H \rightarrow WW^{(*)} \rightarrow \ell\nu\ell\nu$, and $qqH \rightarrow qqWW$. The significance of Higgs signals with the different decay modes in ATLAS are shown in Fig. 12.

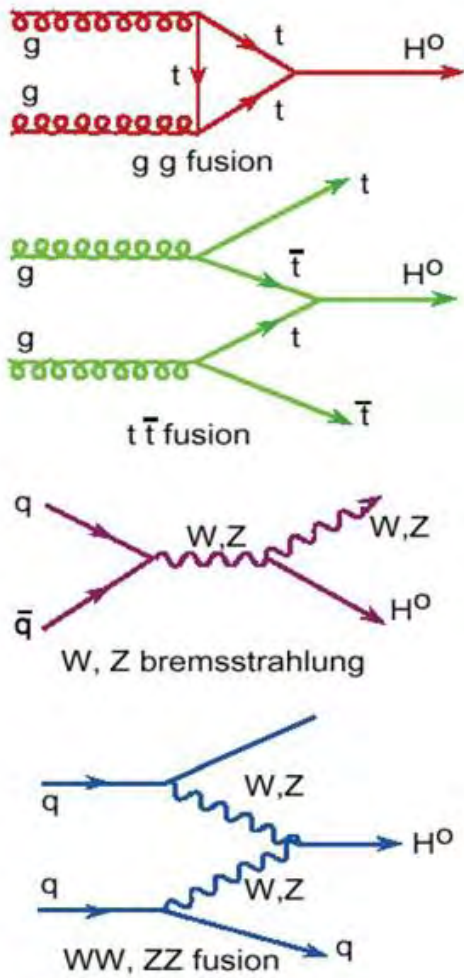


Figure 11. Higgs production through gluon-gluon fusion, top-antitop fusion, W/Z bremsstrahlung, and WW/ZZ fusion.

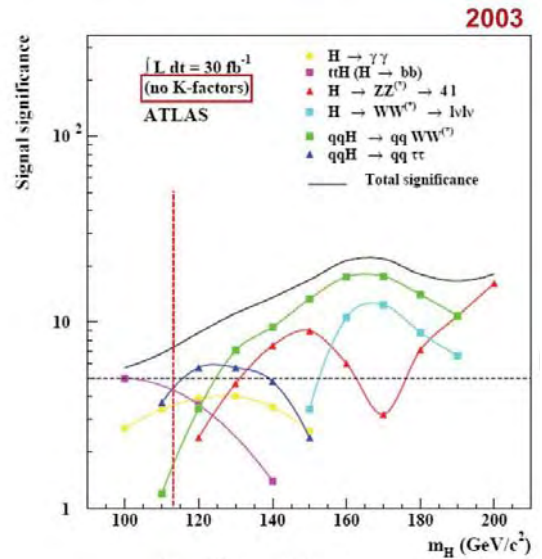


Figure 12. Higgs signal significance in ATLAS in different decay modes as a function of the Higgs mass. Significance S of the signal is defined as $S = N(\text{signal})/\sqrt{N(\text{background})}$. The assumed integrated luminosity is 30 fb^{-1} .

4.2. B Physics

The ATLAS B -physics goals comprise both precision measurements and a search for new physics beyond the Standard Model. One of the CP-violation parameters, called $\sin(2\beta)$, can be measured with a high precision (at the percent level) using time-dependent asymmetry between the decays $B_d^0 \rightarrow J/\psi K_S^0$ and $\bar{B}_d^0 \rightarrow J/\psi K_S^0$. The contributions from a possible new physics phase Θ_{NP} can be distinguished if they contribute at this level or more.

ATLAS will be able to measure a wealth of B -hadron parameters. In particular, measurements of B_s^0 , B_c and b -baryon properties will be highly interesting since the currently operating B -factories at SLAC (US) and KEK (Japan) laboratories cannot produce these particles, and the statistics at the Tevatron will be limited. ATLAS will be able to measure, for example, the $B_s^0 - \bar{B}_s^0$ mixing parameter Δm_s , the lifetime difference between the B_s^0 meson flavour eigenstates $\Delta\Gamma_s/\Gamma_s$, and the weak phase Θ_s of the B_s^0 -meson system with good precision. Properties of the B_c -meson such as mass and lifetime will be measured with high statistics, giving insight to the strong potential binding the heavy quarks together, as well as to the interplay between strong and electroweak effects. b -baryon spectroscopy has just been started at the Tevatron, and ATLAS will continue these measurements, as well as other measurements such as the Λ_b polarization. Finally, the family of very rare decays $B \rightarrow \mu^+ \mu^- (X)$ will give a handle on exploring the new-physics parameter space.

4.3. Mini Black Holes

Some of the New Physics models, *i.e.* models going beyond the current Standard Model, predict the existence of more dimensions than the four we know of (three space dimensions and one time dimension). These new models could for example explain why gravity is so weak (the explanation would be that the gravity is actually as strong as the other forces, but it mainly resides in an unobservable dimension). These models provide a possible solution to the hierarchy problem, since the Planck scale could be close to the electroweak scale if the extra dimensions are taken

into account.

The extra dimension models may allow for the production of mini black holes, if the parton-parton impact parameter would be less than the Schwarzschild radius. These mini black holes would evaporate immediately through Hawking radiation, leading to a spherical production of all types of particles. The signal for mini black hole production would be an excess of spherical events with a high invariant mass.

5. ATLAS current status

In the cavern, common data-taking with a cosmic-ray trigger is serving to test the detector performance. Figure 13 shows a reconstructed cosmic muon in the ATLAS subdetectors.

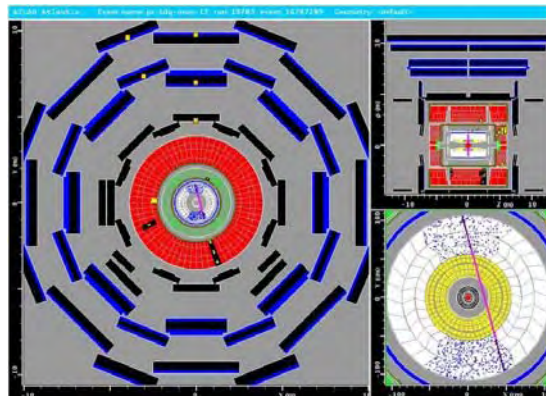


Figure 13. A cosmic muon as seen in the ATLAS subdetectors.

The current turn-on plans for the LHC are as follows. The beam-pipe will be closed in June 2008, followed by first injection of protons into the LHC ring later in June. The first collisions at $\sqrt{s} = 14$ TeV centre-of-mass energy will take place in at the end of summer 2008. November 2007. The first pilot run with a luminosity of about $1 \times 10^{32} \text{ cm}^{-2}\text{s}^{-1}$ should take place before the end of 2008.

REFERENCES

1. W.-M. Yao *et al.*, J. Phys. G: Nucl. Part. Phys. 33 (2006) 1.
Online: <http://pdg.lbl.gov/>
2. ATLAS Detector and Physics Performance Technical Design Report, Vols I and II, CERN/LHCC-99-014 and CERN/LHCC-99-015, 1999.